Deep-Sea Research II 58 (2011) 449–461

Contents lists available at ScienceDirect

Deep-Sea Research II

journal homepage: www.elsevier.com/locate/dsr2

Particulate silica and Si recycling in the surface waters of the Eastern Equatorial Pacific

Mohamed Adjou [a,*], Paul Tréguer [a], Cynthia Dumousseaud [b], Rudolph Corvaisier [a], Mark A. Brzezinski [c], David M. Nelson [a]

[a] Institut Universitaire Européen de la Mer, CNRS, Université Européenne de Bretagne, Technopole Brest-Iroise Place Copernic, Plouzané 29280, France
[b] National Oceanography Centre, Southampton, European Way, Southampton S014 3ZH, United Kingdom
[c] University of California at Santa Barbara, Department of Ecology, Evolution, and Marine Biology, Santa Barbara, CA 93106, United States

ARTICLE INFO

Article history:
Received 9 August 2010
Accepted 9 August 2010
Available online 17 August 2010

Keywords:
The Eastern Equatorial Pacific
Biogenic Silica
Lithogenic Silica
Silicate
Silica net production or dissolution
Si recycling

ABSTRACT

The distributions of biogenic and lithogenic silica concentrations and net silica production rates in the upper 120 m of the Eastern Equatorial Pacific (EEP) were examined in December 2004, on two transects situated at 110°W (4°N to 3°S) and along the equator (110°W to 140°W). Lithogenic silica ($lSiO_2$) was generally <10 nmol Si l^{-1} with maximum concentrations reaching 25 nmol l^{-1} in surface waters. These low concentrations confirm low atmospheric inputs of particulate Si, consistent with reported low inputs of wind-borne material in the EEP. In spite of active upwelling of silicic acid-rich waters the biogenic silica ($bSiO_2$) concentrations were generally low, falling between 100 and 180 nmol Si l^{-1} in the upper 50 m and decreasing to less than 50 nmol Si l^{-1} below ~90 m. Estimates of net $bSiO_2$ production rates revealed that the rate of production exceeded that of dissolution in the upper euphotic layer (0-40 m) along 110°W with net production extending somewhat deeper (60-100 m) to the west along the equator. Net production rates in the surface layer were low, ranging between 5 and 40 nmol Si l^{-1} d^{-1}, consistent with previous observations that diatoms are small contributors to autotrophic biomass in the EEP. Net silica dissolution predominated in the lower euphotic layer (40-120 m), indicating active Si recycling which diminished the strength of the silica pump in this region.

1. Introduction

An upper limit of the contribution of diatoms to the biological carbon pump is set up by the ratio of diatom silica production to its rate of dissolution in surface waters. Thus, determining the level of net silica production in the ocean is a key issue for marine biogeochemistry. The balance between silica production and dissolution in the upper ocean is poorly defined but it is generally thought that about 50% of the silica production in the euphotic zone dissolves in the upper 200 m (Nelson et al., 1995). However, losses from dissolution much greater than 50% have been reported in surface waters both for oligotrophic waters and coastal upwelling regions (review in Nelson et al., 1995), and even for the Southern Ocean (Beucher et al., 2004), one of the three major High Nutrient Low Chlorophyll (HNLC) regions of the world ocean. Such high losses of biogenic silica imply that much of the organic material associated with diatoms is also recycled within the euphotic zone, diminishing the contribution of diatoms to new and export production.

The Eastern Equatorial Pacific (EEP) is another major HNLC region, for which the contribution of diatoms to the biological pump of carbon has not been well documented. The EEP is both a strong carbon dioxide source for the atmosphere and a biological sink for seawater pCO_2 (Tans et al., 1990; Takahashi et al., 2002). This region is well known for its wind-driven upwelling at the equator and for strong atmosphere–ocean interactions. The upward slope of the thermocline to the east brings nutrient-rich deep water toward the surface where it can be entrained to the surface by local upwelling (Chai et al., 1996). As shown by Dugdale and Wilkerson (1998), silicic acid concentrations are consistently lower than those of nitrate in surface waters of the EEP, making it a High Nutrient Low Silicate Low Chlorophyll (HNLSiLC) system. A strong silica pump in the EEP has been postulated by Dugdale et al. (1995) and Dugdale and Wilkerson (1998), by which losses of biogenic silica through dissolution in the surface waters are minor compared to more efficient recycling of nitrogen, driving the system to Si limitation. Thus, primary production due to diatoms would be limited by the influx of silicic acid from below, and net production and export of biogenic silica would be in balance, whereas a significant fraction of nitrogen production would be supported by nitrogen regenerated in the photic layer.

* Corresponding author.
Current address: Center for Macroecology, Evolution, and Climate, Department of Biology, University of Copenhagen, DK-2100 Copenhagen, Denmark.
E-mail address: MAdjou@bio.ku.dk (M. Adjou).

0967-0645/$ - see front matter © 2010 Elsevier Ltd. All rights reserved.
doi:10.1016/j.dsr2.2010.08.002

The export of diatom silica from the surface waters is reflected in the high opal content of the sediments underlying the EEP (Broecker and Peng, 1982). Whereas a significant fraction of those deposits are due to radiolarians (Welling and Pisias, 1998), the export of diatom blooms in the EEP has been documented both on the sea floor and by sediment trap studies (Ragueneau et al., 2000; Honjo et al., 2008). So far however, the fraction of diatom production that is exported, and thus the strength of the silica pump, have not been quantified.

The aims of this study were to constrain the silica cycle and the strength of the silica pump in the EPP by: (1) describing the distribution of silicic acid, biogenic silica ($bSiO_2$) and lithogenic silica ($lSiO_2$) in the 0-150 m layer and (2) estimating the net rate of $bSiO_2$ production or dissolution in the euphotic zone.

2. Material and methods

2.1. Study area and sampling

The "Biocomplexity-1" cruise was conducted from 3 December 2004 to 2 January 2005 aboard the R/V *Roger Revelle*. The cruise consisted of two sections: a section along 110°W longitude from 4°N to 4°S, and an equatorial section from 110°W to 140°W (Fig. 1). We sampled at 13 stations along those two sections. At each station, water sampling was performed at 6 depths (corresponding to 100, 31, 7.5, 5, 0.8 and 0.1% of surface Photosynthetically Available Radiation, PAR) excepted for 4 stations where the sampling was performed for 2 surface depths (100 and 31% PAR). Table 1 shows the station number, location and percentages of PAR and depths of samples. Our main goal was to conduct experiments to measure rates of net silica production (see below) to compliment measures of gross silica production rates using ^{32}Si tracer (see Krause et al., 2011). Due to water volume constraints our measurements were made on separate casts from those other studies. Thus, we also sampled for dissolved and particulate silicon concentrations. Our measurements of biogenic and dissolved silicon complement the larger data set for these parameters collected by Krause et al. (2011). Additional data on net silica production rates were measured on the second cruise in this program in 2005 (Demarest et al., 2011). Measurements of lithogenic silica concentration reported here are unique in that no other research group performed these measurements on either cruise.

2.2. Silicic acid concentrations

Silicic acid concentration [$Si(OH)_4$] was determined manually on board using Mullin and Riley (1955)'s colorimetric method as

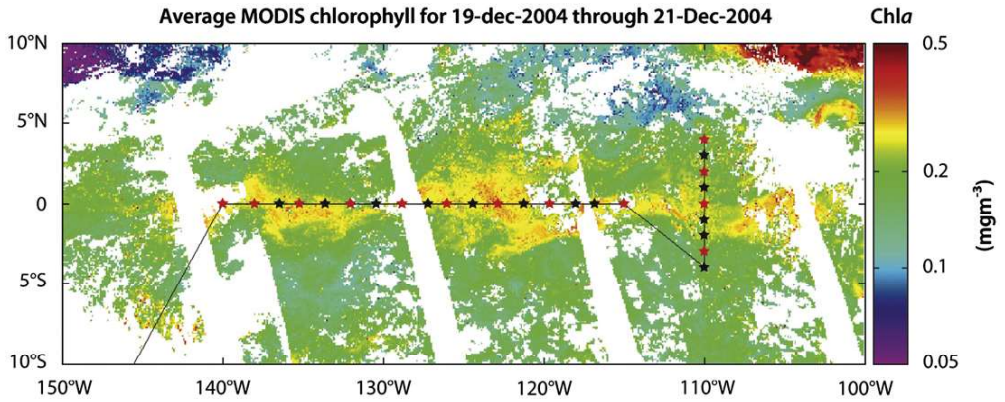

Fig. 1. Location of stations superimposed on a composite of chlorophyll-*a* distribution obtained by satellite during the cruise. Stars indicate the station locations. Red stars represent the stations where measurements of net silica production were performed.

Table 1
Station location and vertical distribution of samples.

Station number	**02**	**04**	**07**	**11**
Longitude (°W)	110	110	110	110
Latitude (°N)	4	2	0	−3
Light penetration (%)	Depth (m)			
100	3	3	0	5
31	23	24	20	21
7.5	51	54	44	47
5	59	62	50	54
0.8	95	100	81	87
0.1	136	138	112	120

Station number	**14**	**16**	**18**	**20**	**22**	**24**	**26**	**28**	**29**
Longitude (°W)	116.8	120	122.8	125.5	128	131.6	135.2	138.7	140
Latitude (°N)	0	0	0	0	0	0	0	0	0
Light penetration (%)	Depth (m)								
100	3	3	3	3	3	3	3	3	3
31	18.6	17	20	20	20	20	20	20	20
7.5	39		44		44		44		43
5	47		51		52		52		51
0.8	75		83		84		83		81
0.1	100		112		114		112		110

modified by Fanning and Pilson (1973). The absorption of the reduced silico-molybdic complex was measured at 810 nm using a PharmaSpec UV.1700 Schimadzu spectrophotometer. Triplicate samples were analysed, using cells of 1 or 10 cm optical paths for optimal transmittance determinations. A typical analytical set comprised triplicates of blanks, of standards made in artificial seawater, and of samples before and after incubation (t_0 and t_f, see below). A reverse order reagent addition was used to determine the blank to subtract from the readings (Brzezinski and Nelson, 1986). The standard deviation was 0.02 μM in the 0 to 25 μM range.

2.3. Biogenic silica concentrations

Biogenic silica concentrations were determined using the sodium hydroxide digestion described by Ragueneau et al. (2000). This protocol dissolves the biogenic silica in sodium hydroxide converting it into orthosilicic acid. The determination of $[Si(OH)_4]$ was done using the manual colorimetric method under conditions similar to those described above. The standard curve was made up in deionized water (DIW) using Na_2SiF_6 (Aminot and Chaussepied, 1983). The blank (including the filter) was 0.6 nmol Si l^{-1} and the limit of detection, determined as three times the standard deviation of the blank, was 0.5 nmol Si l^{-1}.

The biogenic silica concentrations were adjusted for the partial digestion of mineral silica phases during the NaOH digestion by measuring the aluminium (Al) concentration in the digest Ragueneau et al. (2000). Al concentrations in the solution after NaOH attack were determined by Inductively Coupled Plasma – Atomic Emission Spectroscopy, and used to correct the apparent biogenic silica concentrations for any lithogenic silica interference. The ratio Si/Al = 3.9, typical of the aeolian material in this region Duce et al. (1991), was used for mineral Si with a value of 0 assumed for biogenic silica. Calibration was obtained using an aluminium standard solution in the same matrix as the samples (NaOH/HCl for $bSiO_2$ and HF/H_3BO_3 for $lSiO_2$). Blanks were 0.01 in the NaOH/HCl matrix and 0.2 nmol Al l^{-1} in the HF/H_3BO_3 matrix (corresponding to $lSiO_2$ correction of 0.8 nmol Si l^{-1}). The limit of detection was 0.03 and 0.3 nmol l^{-1} for the digests of the biogenic and lithogenic phases, respectively.

2.4. Lithogenic silica concentrations

Lithogenic silica concentrations were determined for the t_0 samples (see below) using the hydrofluoric acid digestion method described by Ragueneau et al. (2000). 0.4 ml of 2.9 M HF was added to the dried filters after the determination of biogenic silica concentrations. Filters were digested for 48 h and 9.6 ml of boric acid (5 g l^{-1}) were added. The use of boric acid was necessary so that HF does not interfere with the $[Si(OH)_4]$ analysis (Eggiman and Betzer, 1976). Concentration of lithogenic silica in the samples was measured using the same colorimetric method as for biogenic silica. The standard curve was made up in the same boric acid/HF matrix as the samples Ragueneau et al. (2000). The blank was 0.6 nmol Si l^{-1} and the limit of detection, determined as three times the standard deviation of the blank, was 1.2 nmol Si l^{-1}.

2.5. Estimates of net production or dissolution of biogenic silica

For each measurement of net silica production, 16 l of sea water were collected at each depth and split in two equal volumes (8 l) in polycarbonate Nalgene® flasks. The first 8-l volume was immediately filtered (sample called t_0), the $[Si(OH)_4]$ of the filtrate and $bSiO_2$ and $lSiO_2$ collected on the filters measured as described above. The second 8-l flask of each pair was placed in a deck incubator fitted with neutral density screens to simulate the light intensity at the depth of collection. All incubators were cooled by running sea-surface water. After a 24 h incubation (sample called t_f) the second 8-l volume from each depth was filtered and analysed for $[Si(OH)_4]$, and $bSiO_2$ in the same manner as used for the t_0 sample. All filtrations were done using 0.6 μm polycarbonate filters. Each filter was dried and stored for measurement of $bSiO_2$ and $lSiO_2$ concentration ashore at the Brest laboratory.

The net rate of silica production or dissolution (ρ_{net}) was estimated by calculating the difference between the biogenic silica concentrations measured at t_0 and t_f:

$$\rho_{net} = [bSiO_2(t_f) - bSiO_2(t_0)]/\Delta t \quad (1)$$

where Δt represents the length of the incubation period. This method requires high precision and accuracy. One potential artefact could come from living or non living siliceous material retained by the polycarbonate walls of the 8-l incubation flasks which could cause the net production rate to be over or underestimated depending upon whether adhesion occurred in the t_0 and t_f sample, respectively.

To constrain the amount of $bSiO_2$ retained on the walls of the incubation flasks an experiment was carried out at the Brest laboratory. A monospecific culture of the diatom *Thalassiosira pseudonana* was diluted with filtered (0.4 μm) seawater from the Iroise Sea (collected on 28 October 2008) and stored in 8 l Nalgene® polycarbonate flasks. Diluted samples were set up to cover the range of $bSiO_2$ concentrations encountered in the photic layer during the Biocomplexity 1 cruise. Three batches of diluted diatom culture at three different $bSiO_2$ concentrations (each in triplicates) were prepared for $bSiO_2$ retention experiments at t_0 and t_f (see below).

Biogenic silica retention experiments at t_0: about fifteen minutes after their preparation, the flasks were vigorously agitated and then filtered through 0.6 μm polycarbonate membranes. The $bSiO_2$ mean concentration (measured in triplicates) at t_0 was 102, 185, and 373 nmol Si l^{-1} in flask 1, 2, and 3 (Table 2), respectively. Four litres of filtered seawater was then poured into each of the three flasks; after vigorous agitation to remove any $bSiO_2$ retained on the polycarbonate walls the seawater samples were filtered through 0.6 μm polycarbonate membranes. The mean $bSiO_2$ amount retained per letter (ε_0), measured in triplicates was 1.7, 2.9, and 6.1 nmol Si l^{-1} in flask 1, 2, and 3 (Table 2), respectively corresponding to a $bSiO_2$ relative retention at t_0 of 1.6–1.7% (Table 2) that was independent of the $bSiO_2$ concentration.

Biogenic silica retention experiments at t_f involved incubating the samples at 15 °C in 8-l flasks, for 24 h under a constant photon flux (200 μE m^{-2} s^{-1}) with a 14/10 h light/dark cycle. At the end of the incubation the t_f samples were treated using exactly the same process as for the t_0 samples. The mean $bSiO_2$ concentration measured in the three flasks at t_f was 147, 271, and 534 nmol l^{-1} in flask 1, 2, and 3 (Table 2). ε_f ,the mean $bSiO_2$ concentrations in the 4 l rinse water was 3.0, 5.6, and 10.3 nmol Si l^{-1} in flask 1, 2,

Table 2
Biogenic silica retention in the 8-l flasks at the initial time (t_0) of sampling and after 24 h of incubation (t_f). Each experiment was done in triplicate. Error terms are standard deviations.

	Flask 1	Flask 2	Flask 3
$[bSiO_2]$ t_0 (nmol Si l^{-1})	102 ± 2	185 ± 8	373 ± 8
ε_0 (nmol Si l^{-1})	1.7 ± 0.4	2.9 ± 0.7	6.1 ± 0.5
$bSiO_2$ retention (%)	1.7 ± 0.4	1.6 ± 0.4	1.6 ± 0.1
$[bSiO_2]$ t_f (nmol Si l^{-1})	147 ± 11	271 ± 18	534 ± 22
ε_f (nmol Si l^{-1})	3.0 ± 0.3	5.6 ± 0.3	10.3 ± 0.5
$bSiO_2$ retention (%)	2.0 ± 0.2	2.0 ± 0.1	1.9 ± 0.1

and 3 (Table 2), respectively for a relative retention of $bSiO_2$ at t_f of 1.9–2.0% for the three flasks (Table 2), a bit higher than for t_0, but still independent of the $bSiO_2$ concentration.

During the cruise we did not determine the amount of $bSiO_2$ retained in each bottle and thus these values may be slightly biased. So the corrected version of Eq. (1) should be:

$$\text{Corrected } \rho_{net} = ([bSiO_2(t_f)+\varepsilon_f]\text{-}[bSiO_2(t_0)+\varepsilon_0)]/\Delta t$$
$$= bSiO_2(t_0)\text{-}bSiO_2(t_0)]+(\varepsilon_f\text{-}\varepsilon_0)]/\Delta t \quad (2)$$

From the above experiment, for the 8-l bottles, the systematic bias ($\varepsilon_f-\varepsilon_0$) is small. For a net production of about 100 nmol Si l^{-1} d^{-1}, this bias is about 2.9% of the net production. Changes between $bSiO_2(t_0)$ and $bSiO_2(t_f)$ were typically much greater than 3%, resulting in clear positive net silica production near the surface and clear net dissolution at depth. This level of analytical uncertainty, however, becomes significant over the depth range encompassing the transition from net production to net dissolution where the changes in $bSiO_2$ approach zero. To illustrate the sensitivity of our measures of net silica production to this error we present the results assuming 0, 5 and 10% retention of $bSiO_2$ on the walls of the 8 l bottles.

2.6. Chlorophyll-a

Chlorophyll-*a* (Chl *a*) was measured using a fluorometric method (JGOFS, 1996). Chl *a* extractions were done in acetone (90%) in darkness at −20 °C for at least 12 h. The analyses were performed using a fluorometer (Turner Designs) that had been calibrated against pure chlorophyll-*a* standards.

3. Results

3.1. Density, temperature and silicic acid

The vertical distributions of σ_t (Fig. 2a and b) and temperature (Fig. 3a and b) in the upper 300 m reveal an asymmetry of the meridional distribution of properties with upwelling prevalent north of the equator. According to Strutton et al. (2011) the 110°W meridional transect passed directly through the centre of a Tropical Instability Vortex (TIV), or the crest of a Tropical Instability Wave (TIW), which perturbed the symmetrical expression of upwelling centred on the equator as indicated by density distribution. The distributions of density and temperature along the zonal section on the equator show a downward slope of the pycnocline (25σ_t isopycnal) and thermocline (20 °C isotherm) from east to west. Salinity (not shown) varied between 34 to 35.5 PSU and shows structure in the isothermal layer indicating that the deep thermocline does not imply a deep mixed layer (Le Borgne et al., 2002).

The distribution of silicic acid (Fig. 4a and b) mirrors that of the physical parameters. The meridional section at 110°W (Fig. 4a) shows surface $[Si(OH)_4]$ ranging from 4.35 to 0.87 μM, decreasing from south to north. Fig. 4b shows that along the equator, from 110°W to 140°W surface $[Si(OH)_4]$ varied from 3.94 to 2.26 μM, generally decreasing from east to west. Fig. 4a and b also show the increase of $[Si(OH)_4]$ with depth, with concentrations rising to 10 to 25 μM below 75 m. The low $[Si(OH)_4]$ to the north on the 110°W section was probably due to a water mass originated from Pacific surface waters as indicated by the low salinity in this region (data not shown, see Strutton et al., 2011).

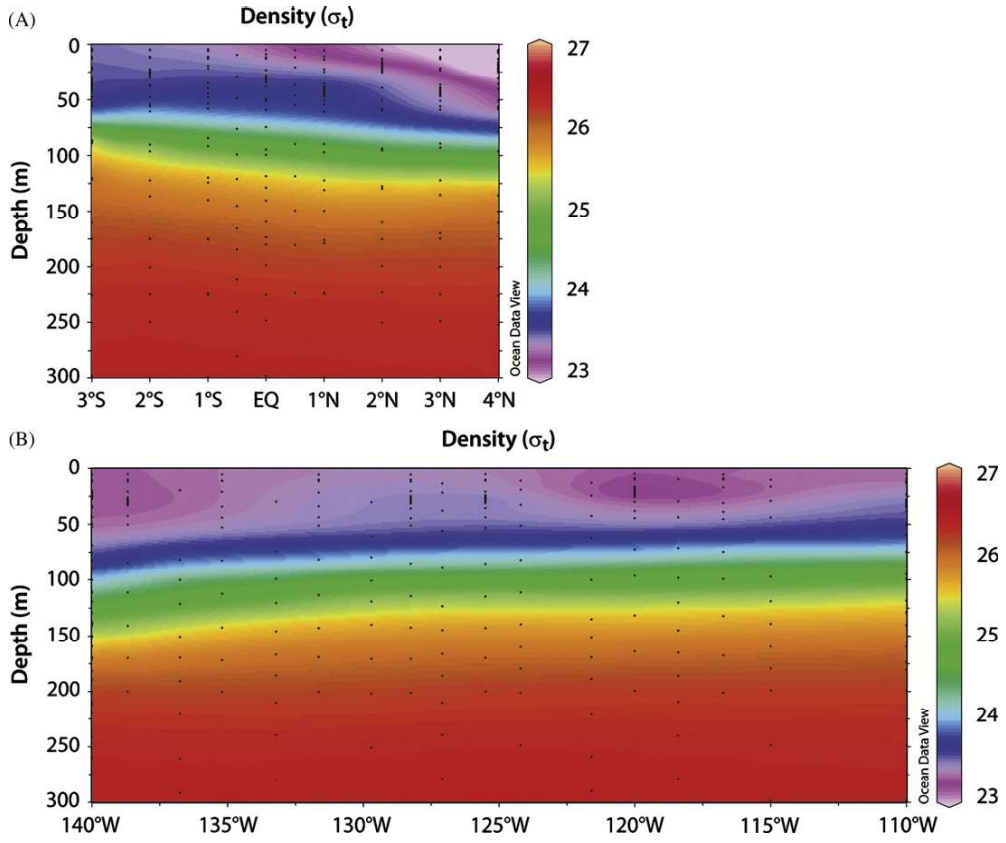

Fig. 2. Latitude-depth (a) and longitude-depth (b) sections of density (σ_t) distribution.

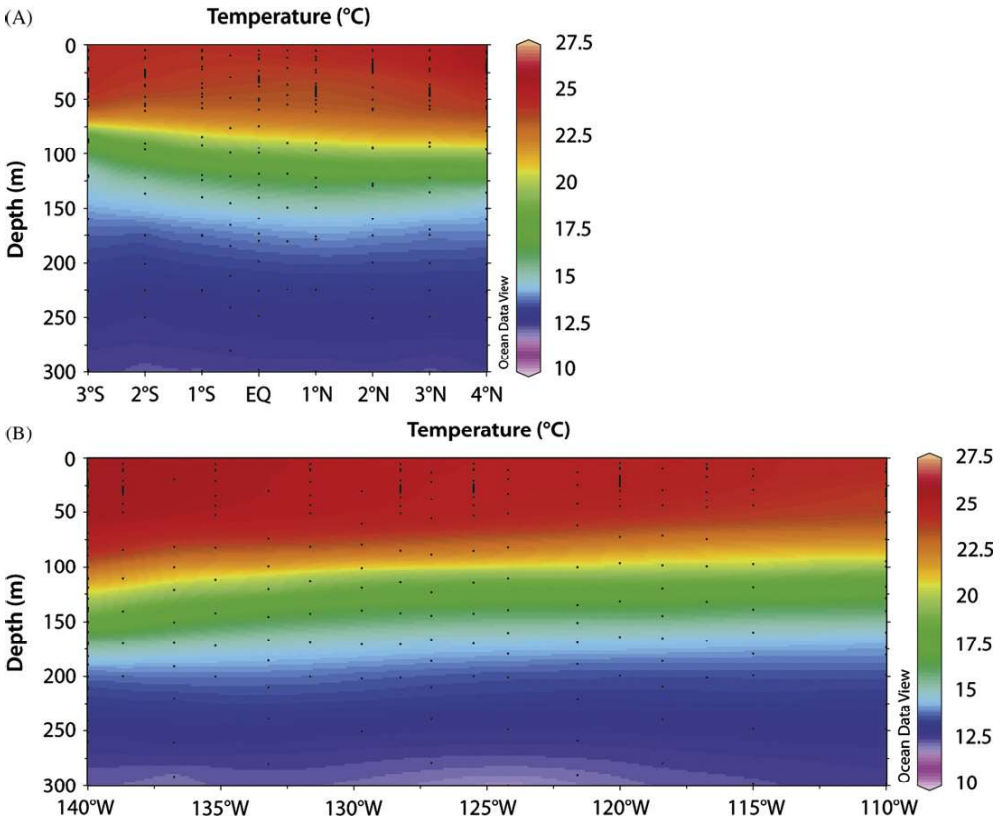

Fig. 3. Latitude-depth (a) and longitude-depth (b) sections of temperature distribution.

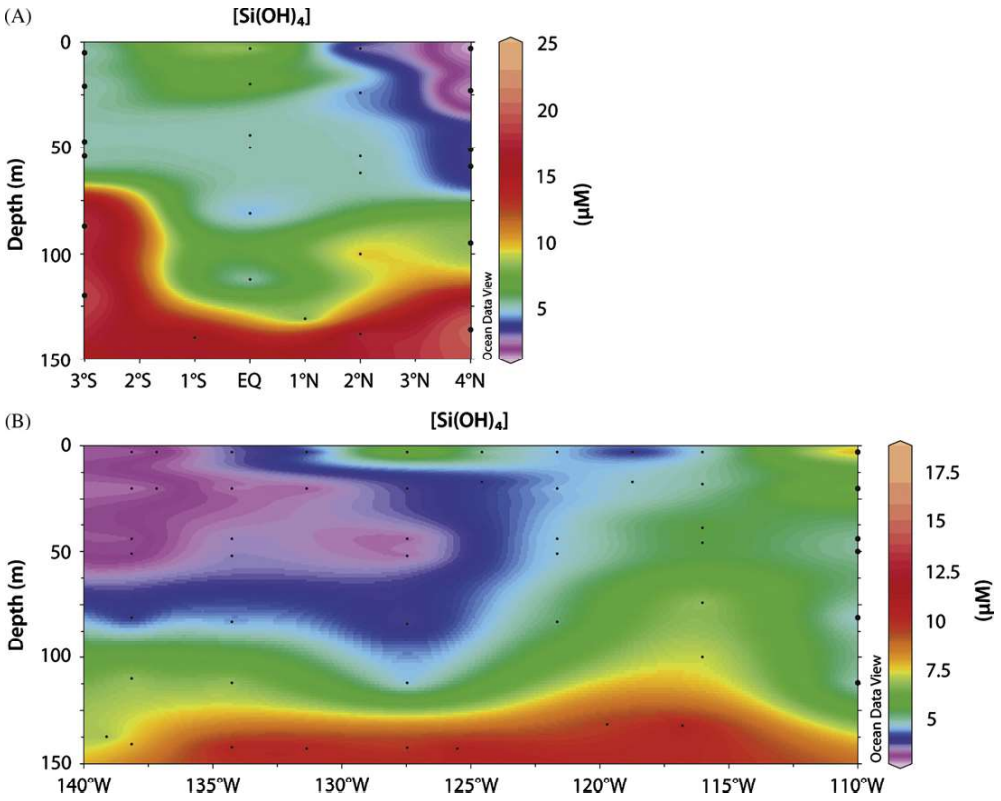

Fig. 4. Latitude-depth (a) and longitude-depth (b) sections of $Si(OH)_4$ distribution.

3.2. Biogenic and lithogenic silica

Fig. 5a and b show the distributions of $bSiO_2$ across the equator at 110°W and along the equator, in the 0-120 m layer. Interestingly these distributions mirror neither those of density or temperature nor that of $[Si(OH)_4]$ indicating that biogenic silica concentration is under control of biological rather than physical processes.

As expected the $bSiO_2$ concentrations were higher in the upper levels of the euphotic zone, which offer more favourable conditions for the growth of diatoms compared to the deeper waters. The meridional transect at 110°W, reveals high mesoscale variability; the southern side of equator, although richer in $[Si(OH)_4]$, is poorer in $bSiO_2$ than waters to the north. A distinct subsurface maximum in $bSiO_2$ at about 20 m was observed between 2°S and 3°N (Fig. 5a). Along the equator, near-surface $bSiO_2$ concentrations increased from 81.4 to >120 nmol l^{-1} from east to west (Fig. 5b). Maximum concentrations (140.7 nmol Si l^{-1}) were measured at 128.3°W coincident with the western edge of a TIW, according to Strutton et al. (2011). Below the euphotic zone $bSiO_2$ decreased with depth with values lower than 50 nmol Si l^{-1} generally measured below 100 m.

Fig. 6a and b show the distribution of $lSiO_2$ in the study area. The $lSiO_2$ concentrations were generally <10 nmol Si l^{-1} (maximum $[lSiO_2]=25$ nmol Si l^{-1}) with the lowest concentrations observed on the equatorial transect near 128°W (5–7 nmol Si l^{-1}). These results are consistent with the low wind-borne dust deposits reported in this region (Duce et al., 1980).

3.3. Net production of biogenic silica

Figs. 7 and 8a show the distribution of the uncorrected ρ_{net} in the study area. Both the meridional (7a) and equatorial (8a) sections show positive ρ_{net} ranging between 0 and 40 nmol Si l^{-1} d^{-1} in near surface waters and negative ρ_{net} (i.e. net silica dissolution), with similar magnitude, at depth. The crossover point from net silica production to net dissolution is generally <50 m along 110°W except for the most southern station at 3°S where it is about 70 m. The crossover from net silica production to net silica dissolution deepens to the west along the equator being <50 m in the east deepening to approximately 100 m to the west. Demarest et al. (2011) measured comparable net production/dissolution during the 2005 Biocomplexity cruise.

Fig. 7b, c and 8b, c show how the distribution of ρ_{net} changes assuming biases ($\varepsilon_f-\varepsilon_0$) of 5 and 10% $bSiO_2$ retention in the incubation bottles. It is clear from this sensitivity analysis that the 5% correction (which is about 2 times larger than our laboratory tests support) causes relatively minor changes to the distributions and to the depth of the crossover from net production to net dissolution. Applying the larger correction factor of 10% has a greater effect, pushing the crossover point to deeper levels in the euphotic zone. Even with the larger correction the depth of zero net production remains shallower than 50 m everywhere along the 110°W section except at 3°S. Along the equator the larger correction would imply that the crossover point is <50 m near 110°W but progressively deepens such that net production occurs throughout the upper 120 m at 140°W. We emphasize that the 10% correction is about 4 times greater than predicted by our laboratory studies. Thus, we believe that the estimates with the zero and five percent correction better define the distribution of net silica production.

3.4. Estimates of silica dissolution rate

At all stations where we measured ρ_{net} (except station 18) the gross rate of $bSiO_2$ production (ρ_{prod}) was measured by Krause et al.

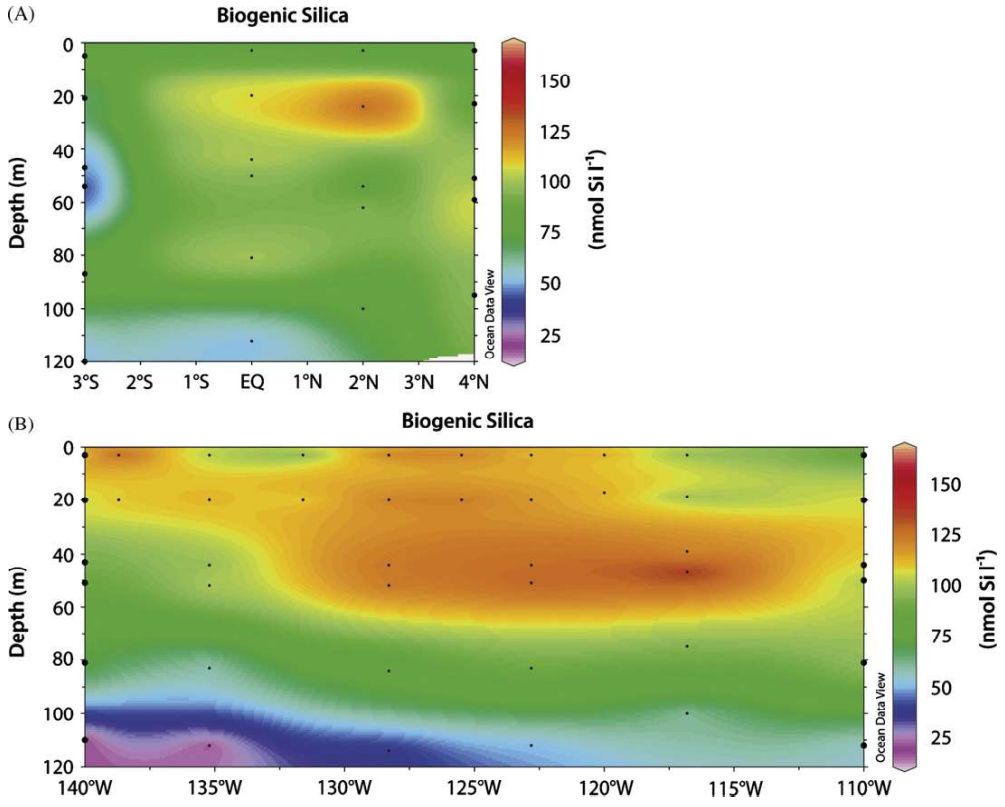

Fig. 5. Latitude-depth (a) and longitude-depth (b) sections of $bSiO_2$ distribution.

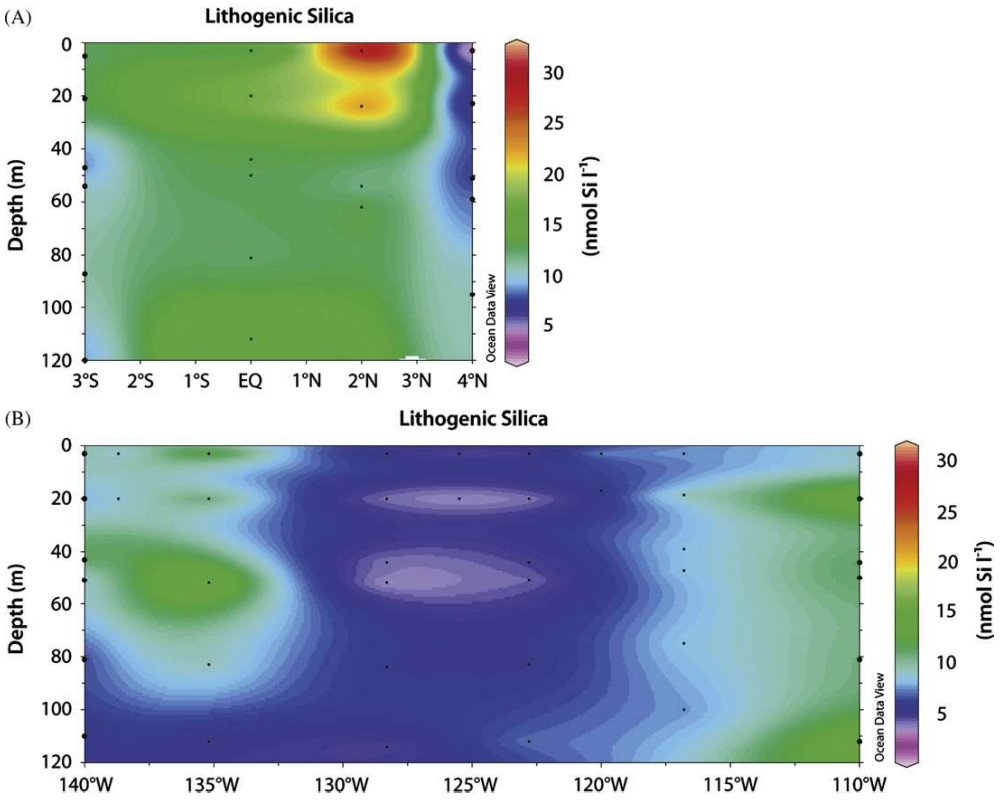

Fig. 6. Latitude-depth (a) and longitude-depth (b) sections of $lSiO_2$ distribution.

(2011) using ^{32}Si tracer and 24 h incubations. Those measurements were made at 8 depths, including the 6 depths at which we measured ρ_{net}. The mean $\int\rho_{prod}$ ($\pm$SD) in the euphotic zone at the 7 stations (Table 3) where we sampled was 1.3 ± 0.6 mmol m^{-2} d^{-1} (meridional mean: 1.4 ± 0.9 mmol m^{-2} d^{-1}; zonal mean: 1.2 ± 0.4 mmol m^{-2} d^{-1}). Water volume constraints required that water for gross and net silica production rate determinations were made on different casts at each station. However, the two casts were made at the same location and depths under comparable conditions. Thus, we use the two rates to estimate the gross silica dissolution rate (ρ_{dis}) at a given depth from equation:

$$\rho_{dis} = \rho_{prod} - \rho_{net} \quad (3)$$

Specific dissolution rate (V_{diss})of biogenic silica in the euphotic zone was calculated from the following equation:

$$V_{dis} = \int \rho_{dis} \left(\int [bSiO_2] \right)^{-1} \quad (4)$$

In the euphotic zone ρ_{dis} varied between 0.7 and 63.9 nmol Si l^{-1} d^{-1}. The mean $\int\rho_{dis}$ ($\pm$SD) over the 7 stations (Table 3) was 1.9 ± 1.0 mmol m^{-2} d^{-1} (meridional mean: 2.6 ± 0.5 mmol m^{-2} d^{-1}: 1.3 ± 0.8 mmol m^{-2} d^{-1}). This calculation failed for five samples over the 42 determinations (Stn 07, 100% I_0 ; Stn 22, 31% I_0; Stn 26, 31 and 5% I_0; Stn 29, 100% I_0) where equation 3 gives negative rates ($\rho_{net} > \rho_{prod}$), for which we do not have any explanation. However, it is likely that short term (hours) differences in diatom biomass or productivity played some role by introducing differences between our cast and those of Krause et al. (2011) for ρ_{prod} and/or ρ_{net}. In the euphotic zone the mean V_{diss} was $(1.9/9.6)=0.20$ d^{-1}.

4. Discussion

Previous studies in the Equatorial Pacific at or west of 180° have shown low concentrations of biogenic silica, with diatoms being minor contributors to primary production (Blain et al., 1999; Leynaert et al., 2001). Our data provide a basis for comparison between the Eastern and the Western Equatorial Pacific, as well as with other HNLC and oligotrophic ecosystems. Our measures of net silica production also provide the first direct evaluation of the potential strength of any 'silicate pump' (Dugdale et al., 1995) in the Equatorial Pacific. We address each of these points below.

4.1. How do the standing stocks of biogenic silica in the Equatorial Pacific compare to other HNLC and oligotrophic ecosystems?

Comparison of our data between 110°Wand 140°W to previous measures from further west in the Central and Western Equatorial Pacific reveal a reasonably consistent standing stock of biogenic silica from 165°E to 110°W with somewhat higher standing stocks of $bSiO_2$ in the eastern part of this zone (Table 4). At 165°E, from 16°S to 6°N, in October 1994, Blain et al. (1999) reported $bSiO_2$ integrated standing stocks that averaged 3 mmol Si m^{-2} in the upper 150 m, peaking at 10 mmol Si m^{-2} at 4°N. At 180°W, from 8°S to 8°N, in November 1996 Leynaert et al. (2001) reported standing stocks averaging 4 mmol Si m^{-2} in the upper 150 m, peaking at 8 mmol Si m^{-2} at equator. At 110°W, from 3°S to 4°N, in December 2004, our study shows that in the integrated biogenic silica concentration in the upper 120 m averaged 9 mmol Si m^{-2}, peaking at 11 mmol Si m^{-2} on the equator. Very similar concentrations of between 8 and 11 mmol Si m^{-2} were

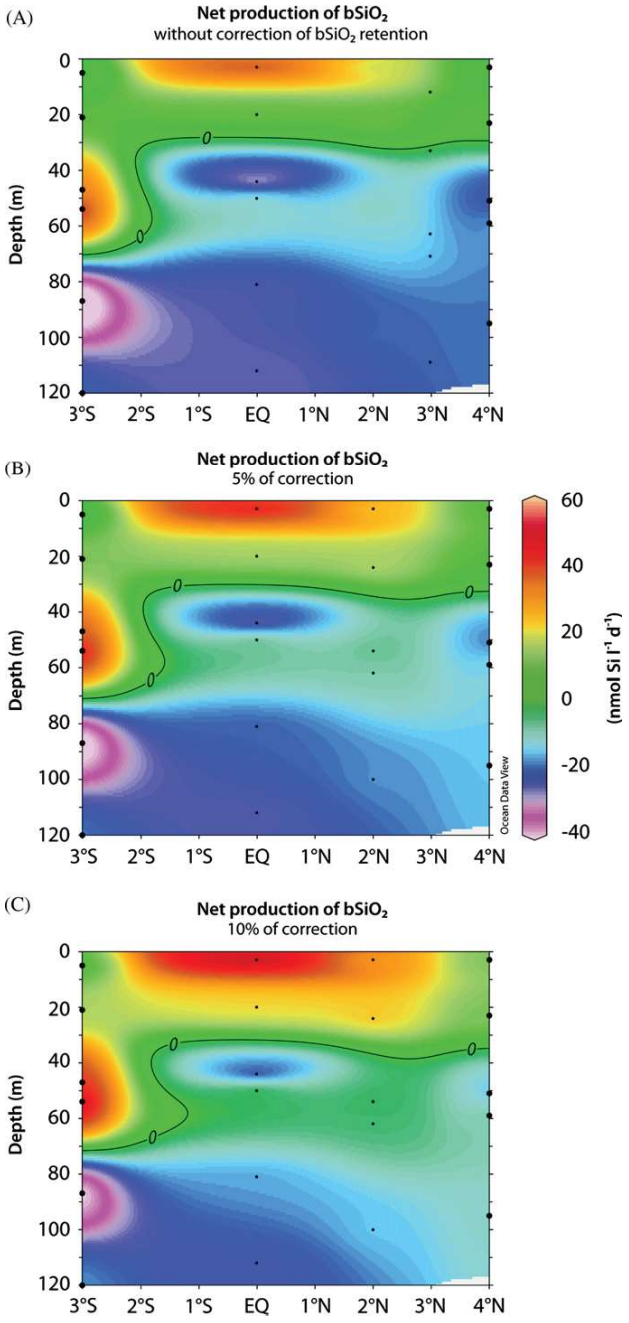

Fig. 7. Meridional distribution of net production of $bSiO_2$: (a) without correction of $bSiO_2$ retention; (b) with 5% correction; (c) with 10% correction.

measured on a second cruise to the region from 140°W to 110°W in 2005 (Krause et al., 2011). This level of consistency is surprising as phytoplankton biomass in equatorial surface waters is significantly impacted by large scale processes like El Niño Southern Oscillation (ENSO), tropical instability waves and Kelvin waves (Foley et al., 1997; Strutton and Chavez, 2000) and the influence of these forcings varied during the cruises when stocks of biogenic silica were accessed. The 165°E FLUPAC cruise (1994) (Blain et al., 1997) took place during an ENSO "neutral scenario" (non El Niño, non La Niña); the EBENE cruise at 180°W (1996) (Leynaert et al., 2001) was performed in similar climatic conditions and our 2004 Biocomplexity 1 cruise (110°W to 140°W) was impacted by a weak El Niño signal (Lyon and Barnston, 2005). Whatever the impact of large scale temporal variability, these three studies show that across a great portion of the Equatorial Pacific, at sites separated by up to 7800 km, the biogenic silica standing stocks in the 0-120 m layer vary only within a reasonably narrow range, averaging between 3 and 9 mmol Si m^{-2}.

Biogenic silica concentrations in the EEP are in the low range for marine waters and similar to those reported for other HNLC and oligothrophic systems (Table 4). The values in the Equatorial Pacific are higher than in oligrotrophic subtropical gyres; Krause et al. (2009) recently established that the average integrated biogenic silica concentration in the upper 120 m at the Bermuda Atlantic Times Series (BATS) site in the Sargasso Sea between 1989 to 2003 was 2.3 mmol m^{-2} (excluding rare mesoscale events during which diatom biomass was exceptionally high). That value is 25 to 50% of integrated biogenic silica concentrations from the EEP. The mean standing stocks across the entire Equatorial Pacific (4 to 9 mmol Si m^{-2}) are similar to the mean reported from the North Pacific Subtropical Gyre (7.1 mmol Si m^{-2}, Table 4). The only other HNLC region with sufficient data for comparison is the Southern Ocean. Although the chlorophyll-*a* stock is about 2 times higher in the EEP than it is the Southern Ocean Permanently Open Ocean Zone during times when no diatom bloom is in progress (Table 4), the standing stock of biogenic silica in the surface layer of the Southern Ocean is about 4 times higher than that in the EEP; when diatom blooms are present in the Southern Ocean the standing stock of biogenic silica is many times greater than this (e.g. Brzezinski et al., 2001). This may reflect a greater dominance of diatoms in the flora of the Southern Ocean (e.g. Arrigo et al., 1998) compared to the Equatorial Pacific where siliceous phytoplankton is a minor contributor to phytoplankton biomass (e.g. Landry et al., 1997).

Biogenic silica concentrations in the surface waters of the EEP are $<10\%$ those of silicic acid. This low standing stock of diatom biomass does not appear to be due to efficient export as Moriceau et al. (2007) showed low rates of $bSiO_2$ export in this region. Alternatively, the low biogenic silica standing stock can be explained by severe grazing of the predominantly small-sized diatoms (Landry et al., 2011; Selph et al., 2011) or low rates of silicic acid uptake in the photic zone. There is experimental evidence that surface silicic acid concentrations limit silicic acid uptake rates in the Equatorial Pacific (Blain et al., 1999; Brzezinski et al., 2008), which would slow rates of both biogenic silica production and silicic acid depletion. However, studies of the kinetics of silicic acid uptake during the Biocomplexity cruises indicate that ambient $[Si(OH)_4]$ are not strongly limiting to Si uptake rates (Brzezinski et al., 2008). Alternatively, low rates of silica production may be the result of Fe limitation of the growth of diatoms (Thomas and Dodson, 1975; Hutchins and Bruland, 1998) or co-limitation by Si and Fe (Brzezinski et al., 2008, 2011). Whereas low rates of silica production would slow rates of silicic acid depletion, the low rates of net silica production measured here suggest that recycling of biogenic silica within the euphotic zone is also important (see below).

Our study and those of Blain et al. (1997, 1999) all reveal the presence of a subsurface biogenic silica maximum ranging from 40 to 180 nmol Si l^{-1} located near the nutricline, coincident or not with a deep chlorophyll maximum (DCM, ranging from 0.25 to 0.34 μg l^{-1}). The DCM can form because of both photoadaptation (light levels between 7.5% and 5% of the surface irradiance, Fig. 9a and b) and growth limitation of diatoms, for instance due to nutrient (including nitrate, silicic acid and/or iron) depletion, within the surface mixed layer. Fig. 9b shows an interesting scenario with a deep $bSiO_2$ maximum (175 nmol Si l^{-1}) at 47 m

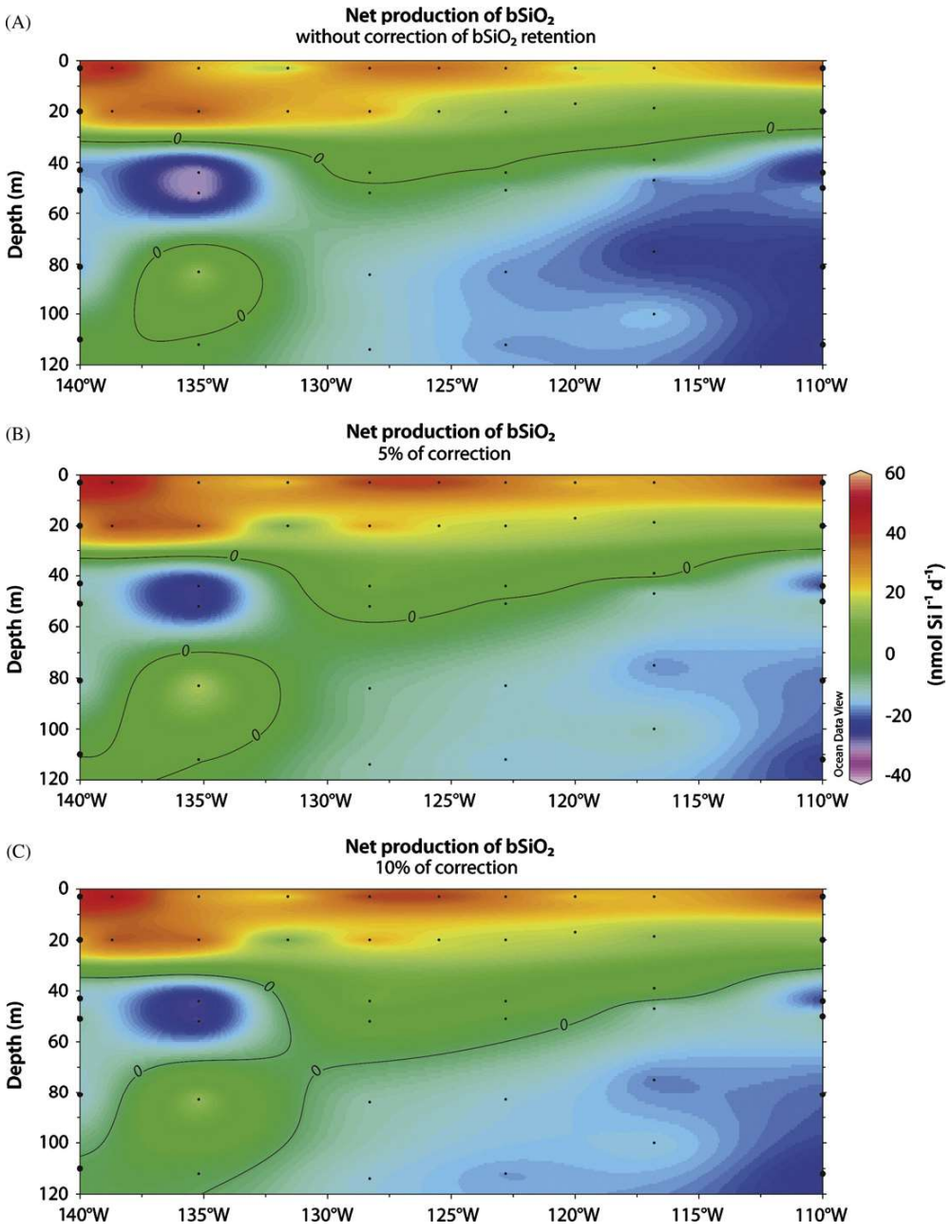

Fig. 8. Zonal distribution of net production of $bSiO_2$: (a) without correction of $bSiO_2$ retention; (b) with 5% correction; (c) with 10% correction.

(5% of surface irradiance), located at the base of the mixed layer, and distinct from the DCM. The spatial mismatch between the vertical distributions of biogenic silica and of chlorophyll-*a* could be explained by accumulation of non-living biogenic silica at the base of the surface mixed layer.

4.2. Net biogenic silica production and Si recycling in surface waters

Along the equator the integrated net production of $bSiO_2$ in the euphotic zone at 6 stations is presented in Fig. 10. In this figure we can observe an east-west trend of net $bSiO_2$ production, with negative net production (i.e. net dissolution) prevailing in the east (110°W to 122°W) and rising gradually to a positive net production in the west of the transect (128°W to 140°W) except for the last station, which seems to have near-zero net production. This distribution of net $bSiO_2$ production is inverse to what we might predict from silicic acid and macronutrient distributions. However, it could be related to iron concentrations which are higher in both surface and subsurface waters near 140°W than near 110°W because the main source of iron to surface waters in the EEP is the Equatorial Undercurrent, an eastward current formed in the West Pacific near New Guinea shelf (Kaupp et al., 2011).

The vertical distribution of net $bSiO_2$ production suggests that the surface waters of the EEP conform to a two-layered system for

Table 3
Integrated biogenic silica net production rates ($\int\rho_{net}$), production rates ($\int\rho_{prod}$)*, dissolution rates ($\int\rho_{dis}$) and dissolution rates corrected from temperature effect ($\int\rho_{dis}$T-cor.)#. At all stations, integration was made using trapezoidal integration (six depths (100, 31, 7.5, 5, 0.8 and 0.1% of surface PAR).

Station	$\int\rho_{net}$ (mmol m^{-2} d^{-1})	$\int\rho_{prod}$ (mmol m^{-2} d^{-1})	$\int\rho_{dis}$ (mmol m^{-2} d^{-1})	$\int\rho_{dis}$T-cor.(mmol m^{-2} d^{-1})
02	−1.71	0.87	2.58	2.13
04	−0.80	2.39	3.18	2.45
07	−1.30	0.84	2.14	1.73
11	−0.32	NA	NA	NA
14	−1.01	1.23	2.45	2.21
18	−0.53	NA	NA	NA
22	0.94	1.71	0.77	0.63
26	0.63	1.37	0.74	0.77
29	−0.47	0.68	1.15	1.13

* Data from Krause et al. (2010).
# For explanations see Section 4.2.

Table 4
Integrated chlorophyll-*a* and biogenic silica in oligotrophic and HNLC zones.

Areas			**$\int$Chl *a* (mg m^{-2})**	**$\int bSiO_2$ (mmol Si m^{-2})**	**References**
Oligotrophic	Sargasso Sea (BATS) (0–120 m)		15.25	2.28	$bSiO_2$: Krause et al. (2009). Chl *a*: Malone et al. (1993)
	North Pacific Subtropical Gyre (0–120 m)		18.2	7.1	Brzezinski et al. (1998)
HNLC	Equatorial Pacific (EP)	Central/West EP (0–150 m)	24.0	4–8	$bSiO_2$: Leynaert et al. (2001). Chl *a*: Blain et al. (1999)
		East EP (0–120 m)	23.5	9.6	This study
	Southern Ocean	Permanently Open Ocean Zone (POOZ) (0–88 m)	15	25.5	Quéguiner et al. (1997)

silica cycling. The upper reaches of the euphotic zone, although not optimal for diatom growth (Leynaert et al., 2001; Hutchins and Bruland, 1998), favoured positive net silica production. However, in the deeper layers silica dissolution prevailed generally (Figs. 7 and 8a). Krause et al. (2011) reported that ρ_{prod} consistently decreases with depth within the euphotic zone, and this was probably a major contributor to the observed transition from net production near the surface to net dissolution below 40–50 m. The transition could also arise if attached bacteria mediated the dissolution of sinking biogenic silica. Observation that bacteria degrade the organic coating surrounding diatom frustules accelerating silica dissolution have been reported from both coastal regions (Biddle and Azam, 1999) and for the Southern Ocean (Beucher et al., 2004). However, bacteria protease activity measured during the cruise reported here did not show significant increase with depth or at the deep $bSiO_2$ maximum (Demarest et al., 2011). During our cruise, intense grazing of diatoms by microzooplankton (consumption of about 60% of diatom daily production), dominated by protists known to engulf and digest individual cells, (Selph et al., 2011) can generate undigested biogenic silica, in suspended matter. This $bSiO_2$ fraction could present a relatively high specific surface area due to the grazed, broken frustules and hence a high dissolution rate (Hurd and Birdwhistell, 1983). Explanations of the vertical transition from net silica production near the surface to net dissolution in the lower euphotic zone based on decreasing production with depth and on increasing dissolution with depth are not mutually exclusive, and both may play a role in the EEP.

The integrated gross rate of biogenic silica production in the euphotic zone in 2004 averaged 1.3 ± 0.6 mmol m^{-2} d^{-1} (estimations from 7 stations; data provided by Krause et al., 2011). The calculated silica dissolution rate was 1.9 ± 1.0 mmol m^{-2} d^{-1} (see results). Thus, the overall dissolution: production (D/P) ratio was 1.4 (1.9 for the meridional transect, 1.0 for the zonal transect), indicating intense, essentially complete dissolution of biogenic silica with the silicic acid requirement in the euphotic zone supplied almost entirely by near-surface silica dissolution. Our estimates of biogenic silica dissolution rates could have been biased too high for samples taken below the mixed layer depth, where the temperature was 4 to 10°C lower than the surface temperature (24–25°C) used for the 24-h on-deck incubations. Using the method of Demarest et al. (2011) we corrected the dissolution rates from temperature effect, using the following equation:

$$\text{corrected } \rho_{dis} = 2.4^{(\Delta T/10)} \times \text{measured } \rho_{dis} \quad (5)$$

where ΔT is the difference between the on-deck incubator and *in situ* temperature for each sample depth. Recalculating the integrated silica dissolution rate using equation (3) gives a mean $\int\rho_{dis}(\pm SD)=1.6\pm0.7$ mmol m^{-2} d^{-1}. So, our best estimate for the mean D/P in the euphotic layer is (1.6/1.3)=1.2 (1.5 for the meridional transect, 0.95 for the zonal transect). This finding is in agreement with the relatively high ratio of biogenic silica dissolution to biogenic silica production in other low-productivity systems. For example, Blain et al. (1999) based on export fluxes measured at 125 m estimated that more than 90% of $bSiO_2$ produced in the euphotic zone of the Western and Central Equatorial Pacific dissolves there. Nelson and Brzezinski (1997), comparing measured gross rates of silica production in the Sargasso Sea with silica export measured by sediment traps at 150 m reported an annual mean D/P ratio of 0.85 for that system.

For the Biocomplexity 2005 cruise in the EEP Demarest et al. (2011) calculated mean D/P of 0.12 and 0.52, for the 0.5°N transect (from 125° to 132.5°W) and along a 140°W transect (from 4°N to 3.25°S), respectively. They concluded that the silica pump was stronger in the upwelling region along the TIW than in the warmer waters of the meridional transect positioned further from the center of the TIW vortex. Obviously, our estimate for mean D/P is higher than Demarest's highest estimate,

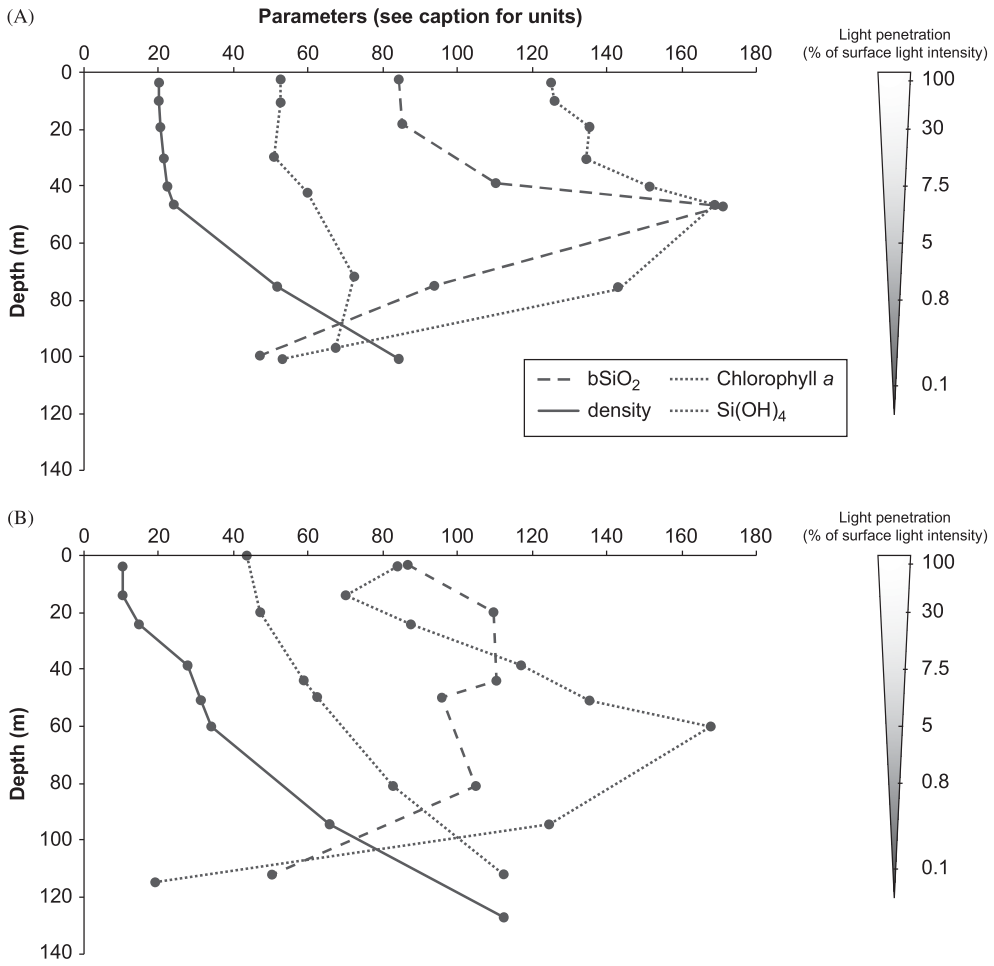

Fig. 9. Profiles of density, $Si(OH)_4$, chlorophyll-*a* and $bSiO_2$. Profiles with various units (Density [$(\sigma$-23)*40 kg m^{-3}]; $Si(OH)_4$ [*12 μM]; Chl a [*0.5 μg m^{-3}]; $bSiO_2$ [nmol Si l^{-1}]) a-Station 14 (0°N-116.8°W): example of coincident deep $bSiO_2$ maximum and DCM. b-Station 07 (0°N-110°W): example of spatial mismatch between deep $bSiO_2$ maximum and DCM.

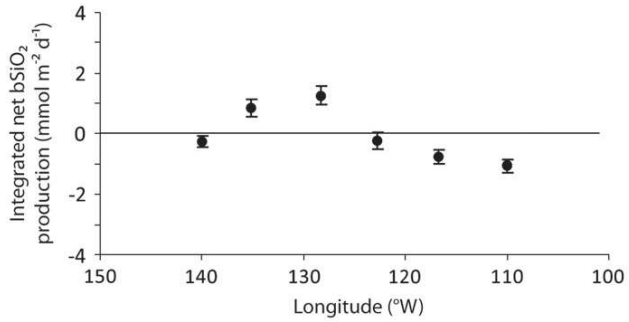

Fig. 10. Integrated net $bSiO_2$ production (euphotic zone) along the equator. Error bars indicate variation between 0% and 5% $bSiO_2$ adsorption (see Section 3 of results).

suggesting that the strength of silica pump may vary temporally in the EEP.

Our results show that active Si recycling occurs in the euphotic zone of the equatorial divergence zone in the Eastern Pacific. This fits well with what has been shown for the Southern Ocean, another HNLC system, where Beucher et al. (2004) and Brzezinski et al. (2001) demonstrated intense Si recycling in the surface waters, at least during austral summer. Such active recycling in the EEP would diminish the fraction of the biogenic silica produced that can be exported beyond the base of the euphotic zone. Low export efficiency for biogenic silica is consistent with the low rates of silica flux shown by Moriceau et al. (2007) and suggests that the silica pump (Dugdale and Wilkerson, 1998) was weak to neutral during the Biocomplexity 2004 cruise. If we look to the silica pump hypothesis for the Equatorial Pacific upwelling zone as formulated by Dugdale and Wilkerson (1998), $bSiO_2$ dissolution was assumed to be negligible as there were no contemporary observations. However, our observations show that dissolution can be of the same general magnitude as biogenic silica production in the system. The intense grazing pressure of diatoms by microzooplankton highlighted by Selph et al. (2011) in the EEP, not considered in the silica pump hypothesis, could be the key ecosystem interaction that results in the observed Si recycling.

5. Conclusion

The low concentrations of lithogenic silica measured in surface waters during this study confirm low aeolian inputs in the Eastern

Equatorial Pacific. Biogenic silica concentrations were low and similar to measurements made to the west previously, suggesting relatively uniform concentrations across a large expanse of the Equatorial Pacific. Our estimates of net silica production show that positive net silica production is confined to the upper 40-50 m of the euphotic zone with net dissolution occurring below. That pattern significantly reduces the potential for the net export of biogenic silica from the upper 100 m and suggests that most silica production in the EEP is supported by locally regenerated $Si(OH)_4$. This would diminish the strength of the silica pump with strong implications as regards the export flux of opal and associated carbon flux to depth.

Acknowledgments

We wish to thank Pete Strutton, Mark Demarest and Jeffrey Krause for fruitful discussions, and Mike Landry and Karen Selph for access to their previously unpublished data. This work was supported by the National Science Foundation Grant OCE0322074 to Oregon State University. *This work benefited also from funds of INSU-CNRS*, and a fellowship from the French Ministry of Research. It is also a contribution to the European Network of Excellence EUR-OCEANS.

References

Aminot, A., Chaussepied, M., 1983. Manuel des analyses chimiques en milieu marin. Centre 516, National pour l'Exploitation des Océans, Brest, France, p. 365.

Arrigo, K.R., Robinson, D.H., Worthen, D.L., Dunbar, R.B., DiTullio, G.R., VanWoert, M., Lizotte, M.P., 1998. Phytoplankton community structure and the drawdown of nutrients and CO_2 in the Southern Ocean. Science 283, 365–367.

Beucher, C., Tréguer, P., Hapette, A.-M., Corvaisier, R., Metzel, N., Pichon, J.-J., 2004. Intense summer Si-recycling in the surface Southern Ocean. Geophysical Research Letters 31 (9. doi:10.1029/2003GL018998.

Biddle, K.D., Azam, F., 1999. Accelerated dissolution of diatom silica by marine bacterial assemblages. Nature 397, 508–512.

Blain, S., Leynaert, A., Tréguer, P., Chretiennot-Dinet, M.J., Rodier, M., 1997. Biomass, growth rates and limitation of Equatorial Pacific diatoms. Deep-Sea Research I 44, 1255–1275.

Blain, S., Tréguer, P., Rodier, M., 1999. Stocks and fluxes of biogenic silica in the western oligotrophic Equatorial Pacific. Journal of Geophysical Research 104, 3357–3367.

Broecker, W.S., Peng, T.H., 1982. Tracers in the Sea. Eldigo Press, Lamont-Doherty Geological Observatory 690pp.

Brzezinski, M.A., Nelson, D.M., 1986. A solvent extraction method for the colorimetric determination of nanomolar concentrations of silicic acid in seawater. Marine Chemistry 19, 139–151.

Brzezinski, M.A., Villareal, T.A., Lipschultz, F., 1998. Silica production and the contribution of diatoms to new and primary production in the Central North Pacific. Marine Ecology Progress Series 167, 89–104.

Brzezinski, M.A., Nelson, D.M., Franck, V.M., Sigmon, D.E., 2001. Silicon dynamics within an intense open-ocean diatom bloom in the Pacific sector of the Southern Ocean. Deep-Sea Research II 48, 3997–4018.

Brzezinski, M.A., Dumousseaud, C., Krause, J.W., Mesasures, C.I., Nelson, D.M., 2008. Iron and silicic acid concentrations together regulate Si uptake in the Equatorial Pacific Ocean. Limnology and Oceanography 53, 875–889.

Brzezinski, M.A., Baines, S., Balch, W.M., Beucher, C., Chai, F., Dugdale, R.C., Krause, J.W., Landry, M.R., Marchi, A., Measures, C.I., Nelson, D.M., Parker, A., Poulton, A., Selph, K.E., Strutton, P., Taylor, A.G., 2011. Twining B.S. Co-limitation of diatoms by iron and silicic acid in the Equatorial Pacific. Deep-Sea Research II 58 (3–4), 493–511.

Chai, F., Lindley, S.T., Barber, R.T., 1996. Origin and maintenance of a high nitrate condition in the Equatorial Pacific. Deep-Sea Research 43, 1031–1064.

Demarest, M.S., Brzezinski, M.A., Nelson, D.M., Krause, J.W., Jones, J.L., Beucher C., 2011. Net biogenic silica production and nitrate regeneration determine the strength of the silica pump in the Eastern Equatorial Pacific. Deep-Sea Research II 58 (3–4), 462–476.

Duce, R.A., Unni, C.K., Ray, B.J., Prospero, J.M., Merrill, J.T., 1980. Long-range atmospheric transport of soil dust from Asia to the tropical North Pacific: temporal variability. Science 209, 1522–1524.

Duce, R.A., Liss, P.S., Merrill, J.T., Atlas, E.L., Buat-Menard, P., Hicks, B.B., Miller, J.M., Prospero, J.M., Arimoto, R., Church, T.M., Ellis, W., Galloway, J.M., Hansen, L., Jickells, T.D., Knap, A.H., Reinhardt, K.H., Schneider, B., Soudine, A., Tokos, J.J., Tsunogai, S., Wollast, R., Zhou, M., 1991. The atmospheric input of trace species to the world ocean. Global Biogeochemcal Cycles 5, 193–259.

Dugdale, R.C., Wilkerson, F.P., Minas, H.J., 1995. The role of a silicate pump in driving new production. Deep-Sea Research I 42, 697–719.

Dugdale, R.C., Wilkerson, F.P., 1998. Silicate regulation of new production in the Equatorial Pacific upwelling. Nature 391, 270–273.

Eggiman, D.W., Betzer, P.R., 1976. Decomposition and analysis of refractory oceanic suspended materials. Analytical Chemistry 48, 866–890.

Fanning, K.A., Pilson, M.E.Q., 1973. On the spectrophotometric determination of dissolved silica in natural waters. Analytical Chemistry 45, 136–140.

Foley, D.G., Dickey, T.D., McPhaden, M.J., Bidigare, R.R., Lewis, M.R., Barber, R.T., Lindley, S.T., Garside, C., Manov, D.V., McNeil, J.D., 1997. Longwaves and primary productivity variations in the Equatorial Pacific at 0°, 140°W. Deep-Sea Research II 44, 1801–1826.

Honjo, S., Manganini, S.J., Krishfield, R.A., Francois, R., 2008. Particulate organic carbon fluxes to the ocean interior and factors controlling the biological pump: a synthesis of global sediment trap programs since 1983. Progress in Oceanography 76, 217–285.

Hurd, D.C., Birdwhistell, S., 1983. On producing a general model for biogenic silica dissolution. American Journal of Science 283, l-28.

Hutchins, D.A., Bruland, K.W., 1998. Iron-limited diatom growth and Si:N uptake in a coastal upwelling regime. Nature 393, 561–564.

JGOFS, 1996. Protocols for the Joint Global Ocean Flux Study (JGOFS) core measurements. Scientific Committee on Oceanic Research, International Council of Scientific Unions, Intergovernmental Oceanographic Commission, Bergen, Norway, 170pp.

Kaupp, L.J., Measures, C.I., Selph, K.E., Mackenzie, F.T., 2011. The distribution of dissolved Fe and Al in the upper waters of the Eastern Equatorial Pacific. Deep-Sea Research II 58 (3–4), 296–310.

Krause, J.W., Nelson, D.M., Brzezinski, M.A., 2011. Biogenic silica production and the diatom contribution to primary production and nitrate uptake in the Eastern Equatorial Pacific Ocean. Deep-Sea Research II 58 (3–4), 434–448.

Krause, J.W., Lomas, M.W., Nelson, D.M., 2009. Biogenic silica at the Bermuda Atlantic Time-series Study site in the Sargasso Sea: Temporal changes and their inferred controls based on a 15-year record. Global Biogeochemical Cycles 23, GB3004. doi:10.1029/2008GB003236.

Landry, M.R., Barber, R.T., Bidigare, R., Chai, F., Coale, K.H., Dam, H.G., Lewis, M.R., Lindley, S.T., McCarthy, J.J., Roman, M.R., Stoecker, D.K., Verity, P.G., White, J.R., 1997. Iron and grazing constraints on primary production in the Central Equatorial Pacific: an EqPac synthesis. Limnology and Oceanography 42, 405–418.

Landry, M.R., Selph, K.E., Taylor, A.G., Décima, M., Balch, W.M., Bidigare, R.R., 2011. Phytoplankton growth, grazing and production balances in the HNLC Equatorial Pacific. Deep-Sea Research II 58 (3–4), 524–535.

Le Borgne, R., Barber, R.T., Delcroix, T., Inoue, H.Y., Mackey, D., Rodier, M., 2002. Pacific warm pool and divergence: temporal and zonal variations on the equator and their effects on the biological pump. Deep-Sea Research II 49, 2471–2512.

Leynaert, A., Tréguer, P., Lancelot, C., Rodier, M., 2001. Silicon limitation of biogenic silica production in the Equatorial Pacific. Deep-Sea Research I 35, 639–660.

Lyon, B., Barnston, A.G., 2005. The evolution of the weak "El Nino" of 2004–2005. US CLIVAR Variations, 3, 〈http://www.usclivar.org/publications.html#V3N2〉.

Malone, T.C., Pike, S.E., Conley, D.J., 1993. Transient variations in phytoplankton productivity at the JGOFS Bermuda time series station. Deep-Sea Research I 40, 903–924.

Moriceau, B., Garvey, M., Ragueneau, O., Passow, U., 2007. Evidence for reduced biogenic silica dissolution rates in diatom aggregates. Marine Ecology Progress Series 333, 129–142.

Mullin, J.B., Riley, J.P., 1955. The spectrophotometric determination of silicate-silicon in natural waters with special reference to sea water. Analytica Chimica Acta 12, 162–170.

Nelson, D.M., Tréguer, P., Brzezinski, M.A., Leynaert, A., Queguiner, B., 1995. Production and dissolution of biogenic silica in the ocean: revised global estimates, comparison with regional data and relationship to biogenic sedimentation. Global Biogeochemical Cycles 9, 359–372.

Nelson, D.M., Brzezinski, M.A., 1997. Diatom growth and productivity in an oligotrophic midocean gyre: a 3-yr record from the Sargasso Sea near Bermuda. Limnology and Oceanography 42, 473–486.

Quéguiner, B., Tréguer, P., Peeken, I., Scharek, R., 1997. Biogeochemical dynamics and the silicon cycle in the Atlantic sector of the Southern Ocean during austral spring 1992. Deep-Sea Research II 44, 69–89.

Ragueneau, O., Treguer, P., Leynaert, A., Anderson, R.F., Brzezinski, M.A., DeMaster, D.J., Dugdale, R.C., Dymond, J., Fischer, G., Francois, R., Heinze, C., Maier-Reimer, E., Martin-Jezequel, V., Nelson, D.M., Quéguiner, B., 2000. A review of the Si cycle in the modern ocean: recent progress and missing gaps in the application of biogenic opal as a paleoproductivity proxy. Global and Planetary Change 26, 317–365.

Selph, K.E., Landry, M.R., Taylor, A., Yang, E.J., Measures, C.I., Yang, J.J., Stukel, M., Christensen, S., Bidigare, R.R., 2011. Spatially-resolved taxon-specific phyto-plankton production and grazing dynamics in relation to iron distributions in the Equatorial Pacific between 110°W and 140°W. Deep-Sea Research II 58 (3–4), 358–377.

Strutton, P.G., Chavez, F.P., 2000. Primary productivity in the Equatorial Pacific during the 1997–98 El Niño. Journal of Geophysical Research 105 (C11), 26089–26101.

Strutton, P., Palacz, A., Dugdale, R.C., Chai, F., Marchi, A., Parker, A., Hogue, V., Wilkerson, F.P., 2011. The impact of Equatorial Pacific tropical instability waves on hydrography and nutrients: 2004–2005. Deep-Sea Research II 58 (3–4), 284–295.

Takahashi, T., Sutherland, S.C., Sweeney, C., Poisson, A., Metzl, N., Tilbrook, B., Bates, N., Wanninkhof, R., Feely, R.A., Sabine, C., Olafsson, J., Nojiri, Y., 2002. Global sea–air CO_2 flux based on climatological surface ocean pCO_2, and seasonal biological and temperature effect. Deep-Sea Research II 49, 1601–1622.

Tans, P.P., Fung, I.Y., Takahashi, T., 1990. Observational constraints on the global atmospheric CO_2 budget. Science 247, 1431–1438.

Thomas, W.H., Dodson, A.N., 1975. On silicic acid limitation of. diatoms in near-surface waters of the Eastern Tropical Pacific Ocean. Deep-Sea Research 22, 671–677.

Welling, L.A., Pisias, N.G., 1998. Radiolarian fluxes, stocks, and population residence times in surface waters of the Central Equatorial Pacific. Deep-Sea Research I 45, 639–671.